J Mol Model (2015) 21: 156
DOI 10.1007/s00894-015-2690-5

ORIGINAL PAPER

Understanding the comparative molecular field analysis (CoMFA) in terms of molecular quantum similarity and DFT-based reactivity descriptors

Alejandro Morales-Bayuelo[1] · **Ricardo A. Matute**[2] · **Julio Caballero**[1]

Received: 30 January 2015 / Accepted: 27 April 2015 / Published online: 28 May 2015

Abstract The three-dimensional quantitative structure-activity relationship (3D QSAR) models have many applications, although the inherent complexity to understand the results coming from 3D-QSAR arises the necessity of new insights in the interpretation of them. Hence, the quantum similarity field as well as reactivity descriptors based on the density functional theory were used in this work as a consistent approach to better understand the 3D-QSAR studies in drug design. For this purpose, the quantification of steric and electrostatic effects on a series of bicycle [4.1.0] heptane derivatives as melanin-concentrating hormone receptor 1 antagonists were performed on the basis of molecular quantum similarity measures. The maximum similarity superposition and the topo-geometrical superposition algorithms were used as molecular alignment methods to deal with the problem of relative molecular orientation in quantum similarity. In addition, a chemical reactivity analysis using global and local descriptors such as chemical hardness, softness, electrophilicity, and Fukui functions, was developed. Overall, our results suggest that the application of this methodology in drug design can be useful when the receptor is known or even unknown.

Keywords Chemical reactivity descriptors · Comparative molecular field analysis (CoMFA) · Density functional theory (DFT) · Melanin-concentrating hormone receptor 1 (MCH-R1) · Molecular quantum similarity (MQS) · 3D-QSAR

Introduction

Since the birth of computer-aided drug design in the 1960s, the computational techniques in drug discovery have been largely implemented in academia and industry. In particular, the methodologies developed in the framework of quantum chemistry to analyze biological activity data from different sets of molecules provide relevant information to describe 3D structure-activity relationships in a quantitative manner, i.e., via comparative molecular field analysis (CoMFA) [1]. In this sense, the density functional theory (DFT), which has its roots in the Hohenberg-Kohn theorems (research leading to the Nobel Prize for Walter Kohn in 1998) [2], becomes a fertile field to explore novel approaches for CoMFA modeling. In the present work, the DFT of chemical reactivity (the so-called conceptual DFT) is used in combination with the molecular quantum similarity (MQS) approach introduced by Carbó and co-workers [3] in order to improve interpretation of a CoMFA 3D-QSAR [4] analysis of a set of molecules that are melanin-concentrating hormone receptor 1 (MCH-R1) antagonists.

Nowadays, obesity can be considered as a chronic disease with serious implication and with a steady increase in cases around the world [5]. The most common causes are a combination of excessive food energy intake, lack of physical activity, and genetic background, among others [6, 7]. The World Health Organization (WHO) has defined obesity as a body mass index (BMI), i.e., weight in kilograms divided by the height square in meters, exceeding 30 kg/m^2 [8–13]. For all these reasons, the search for new drugs to treat obesity is an area of intense interest around the world.

Electronic supplementary material The online version of this article (doi:10.1007/s00894-015-2690-5) contains supplementary material, which is available to authorized users.

✉ Alejandro Morales-Bayuelo
alejandr.morales@uandresbello.edu

[1] Centro de Bioinformática y Simulación Molecular (CBSM), Universidad de Talca, 2 Norte 685, Casilla 721, Talca, Chile

[2] Departamento de Química, Facultad de Ciencias, Universidad de Chile, Casilla 653, Santiago, Chile

In recent years, experimental and theoretical works have been devoted to the study of the melanin concentrating hormone (MCH) [14], which has become an important target for the treatment of obesity [15]. Two MCH receptors have been characterized recently, namely MCH-R1 and MCH-R2 [16, 17]. These two receptors have approximately 38 % homology. The receptor MCH-R1 has received more attention, probably due to the fact that it is expressed in rodents [15].

In order to study the selectivity sites in a series of bicycle [4.1.0] heptane derivatives as melanin-concentrating hormone receptor 1 (MCH-R1) antagonists, we performed quantification of steric and electronic effects using the MQS field together with conceptual DFT-based reactivity descriptors [18–20] such as the chemical hardness, softness, electrophilicity, and Fukui functions.

In the QSAR studies, the basic assumption for all molecule based hypotheses is that similar molecules have similar activities (structure–activity relationship (SAR) principle). The underlying problem is, therefore, how to define a small difference on a molecular level, since each kind of activity, e.g., selectivity or reactivity ability to receptor R1 or R2 in MCH antagonists, might depend on such structural differences. For this reason, we used hybrid methodologies, combining the quantum similarity field and chemical reactivity on DFT to obtain the distinctive patterns (steric and electronic effects) to describe reactivity abilities in this molecular set. In this sense, we suggest that the quantum similarity indexes and chemical reactivity descriptors in the DFT context can indeed provide valuable information on the structural and electronic properties. Hence, both the correlation and complementarity between the chemical reactivity and quantum similarity on the 3D-QSAR studies were analyzed.

Theory and computational details

Molecular quantum similarity indexes

We have considered that the MQS field is based on the same principle as the 3D QSAR studies, i.e., "similar molecules tend to have similar behavior". The similarity indexes were introduced by Carbó and co-workers (see reviews on quantum similarity of refs. [18–24]), and they define the quantum similarity measure Z_{AB} between compounds A and B, with electron density $\rho_A(r_1)$ and $\rho_B(r_2)$ respectively, based on the idea of the minimizing of the expression for the Euclidean distance as:

$$D_{AB}^2 = \int |\rho_A(r) - \rho_B(r)|^2 dr = \int (\rho_A(r_1))^2 dr_1 + \int (\rho_B(r_2))^2 dr_2 - 2\int \rho_A(r_1)\rho_B(r_2) dr_1 dr_2 = Z_{AA} + Z_{BB} - 2Z_{AB} \quad (1)$$

Overlap integral involving the Z_{AB} between the electronic density of compounds A and B, Z_{AA} and Z_{BB} are the self-similarity of compounds A and B [25].

The most common quantum similarity index is the one generalized by the cosine, introduced by Carbó et al. [25]. This index can be expressed mathematically as:

$$I_{AB} = \frac{\int \rho_A(r_1)\rho_B(r_2) dr_1 dr_2}{\sqrt{\int (\rho_A(r_1))^2 dr_1 \int (\rho_B(r_2))^2 dr_2}} \quad (2)$$

or using the elements of Z in an operator (Ω).

$$I_{AB} = \frac{Z_{AB}(\Omega)}{\sqrt{Z_{AA}(\Omega) Z_{BB}(\Omega)}} \quad (3)$$

In Eq. (3), the index is mathematically defined in the interval (0,1] where 1 is self-similarity, and where only the measures of "shape similarity" are included. Another alternative is the Hodgkin-Richards index [25], which appears naturally when using the arithmetic mean and can be defined mathematically as:

$$I_{AB} = \frac{2Z_{AB}(\Omega)}{Z_{AA}(\Omega) + Z_{BB}(\Omega)} \quad (4)$$

where (Ω) is the operator for the measurement of quantum similarity. Equation (4) shows another way to make quantum similarity measures (QSM), however the Carbó index is widely used and for that reason it is also used in this study.

The hirshfeld approach to study the local quantum similarity

Due to that the molecules studied have a central nitrogen atom, we analyzed the local similarity (Fig. 1a)) using the Hirshfeld approach, since this approach is supported by a robust theoretical framework, and also considering that for molecules with many atoms, the choice of a reasonable partitioning scheme is crucial.

The Hirshfeld approach was developed in 1977 [27]. This approach is based on partitioning of the electronic density $\rho(r)$ in contributions $\rho_{N^1}(r)$.

These contributions are proportional to the weight $w_N(r)$ of the electronic density of the isolated compound in the so-called *promolecular density* [28, 29]. This weight is defined as the ratio of the electronic density of the isolated atom and the superposition of the densities of all atoms isolated in the same position of the compound. The promolecular density is defined as:

$$\rho_{N^1}^{Prom}(r) = \sum_x \rho_x^0(r) \quad (5)$$

The contribution of nitrogen atom (N) in the electronic density in ρA(r) for molecule A is obtained as

$$\rho_{N^1}(r) = w_N(r)\rho_A(r). \quad (6)$$

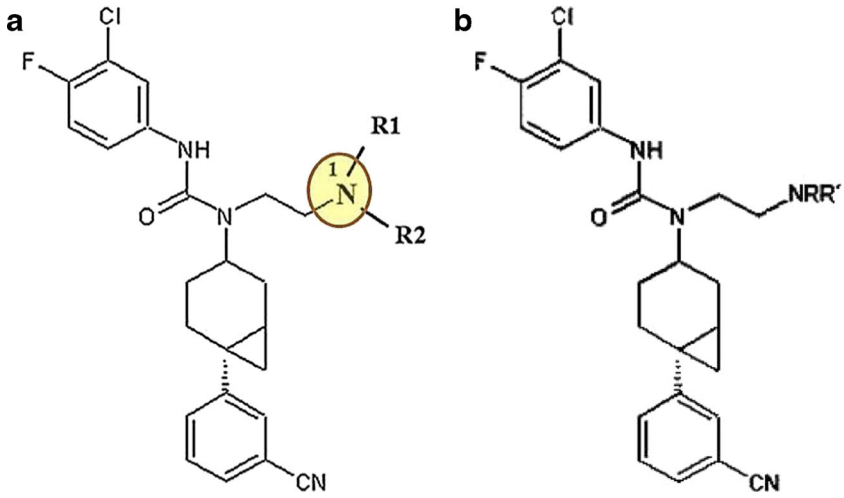

Fig. 1 **a** The nitrogen atom labeled is used in the Hirshfeld approach to calculate the local quantum similarity. **b** Molecular recognition skeleton used for the molecular alignment with NRR' of Table 1

Whereby the weight ($w_N(r)$) is obtained as:

$$w_{N^1}(r) = \frac{\rho^0_{N^1}}{\sum_x \rho^0_x(r)} \tag{7}$$

Where $\rho^0_N(r)$ is the electronic density of the isolated nitrogen atom N [30], which allows to include steric and electrostatic effects from nitrogen atoms in the molecular set.

Thus, the contribution atomic nitrogen atom (N^2) in another molecule, B, is obtained as:

$$\rho_{N^2,B}(r) = w_{N^2}(r)\rho_B(r) \tag{8}$$

with

$$w_{N^2,B} = \frac{\rho^0_{N^2,B}(r)}{\sum_x \rho^0_x(r)} \tag{9}$$

So we can write the contribution of the asymmetric nitrogen atom products $\rho_A(r)\rho_B(r)$ as:

$$\rho_{N,AB}(r) = w_{N,AB}(r)\rho_A(r)\rho_B(r) \tag{10}$$

So that we can express the numerator Z_{AB} Carbó index (Eq. 3) as:

$$Z^{Local,N}_{A,B} = \frac{Z_{AB}}{\sqrt{Z_{AA}Z_{BB}}} = \frac{\iint w_{N,AB}\rho_A(r)\rho_B(r)dr_A dr_B}{\sqrt{\left(\int w_{N,A}(r)\rho_A(r)dr\right)^2\left(\int w_{N,B}(r)\rho_B(r)dr\right)^2}} \tag{11}$$

where we can see the global index (Eq. 3) as local contributions.

Reactivity indexes within the DFT framework

Generally, the similarity indexes (and specially the Coulomb index) can be related to electronic factors associated with chemical reactivity. Hence, we used the traditional formalism associated to the traditional DFT in order to better understand the chemical reactivity of the molecular set under study.

Using the Hohenberg–Kohn theorems [18–20]:

$$\begin{aligned} E &= T[\rho] + V_{ee}[\rho] + V_{ne}[\rho] \\ &= \int \rho(r)\upsilon(r)dr + F_{HK}\ [\rho] \end{aligned} \tag{12}$$

Therefore, when differentiating the total energy, we get:

$$dE = \left(\frac{\partial E}{\partial N}\right)_\upsilon dN + \int \left(\frac{\delta E}{\delta \upsilon(r)}\right)_N \delta\upsilon(r)dr \tag{13}$$

From Eq. (13), we obtain:

$$\left(\frac{\delta E}{\delta \upsilon(r)}\right)_N = \rho(r)\ , \quad \left(\frac{\partial E}{\partial N}\right)_\upsilon = \mu \tag{14}$$

In Eq. 14, we defined (μ) as chemical potential. In this way, Eq. 13 takes the form:

$$dE = \mu dN + \int \rho(r)\delta\upsilon(r)dr \tag{15}$$

Taking the differentiation of Eq. 15, we obtain:

$$\begin{aligned} d^2E = &\left(\frac{\partial \rho(r)}{\partial N}\right)_\upsilon dN + \int \left(\frac{\delta\rho(r)}{\delta\upsilon(r)}\right)_N \delta\upsilon(r)dr \\ &+ \left(\frac{\partial \mu}{\partial N}\right)_\upsilon dN + \int \left(\frac{\delta\mu}{\delta\upsilon(r)}\right)_N \delta\upsilon(r)dr \end{aligned} \tag{16}$$

of Eqs. 15 and 16, is defined:

$$\left(\frac{\partial\rho(r)}{\partial N}\right)_\upsilon = \left(\frac{\partial\delta E}{\partial N\delta\upsilon(r)}\right) = \left(\frac{\delta\mu}{\delta\upsilon(r)}\right)_N = f(r) \tag{17}$$

where $f(r)$ is known as the Fukui function.

Finally, using the Taylor expansion to the total energy, we obtain:

$$E[N+\Delta N, v(r)+\delta v(r)] = E^0[N, v(r)] + \left(\frac{\partial E}{\partial N}\right)_v \Delta N + \frac{1}{2}\left(\frac{\partial^2 E}{\partial N^2}\right)_v \Delta N^2 + \int \left(\frac{\delta E}{\delta v(r)}\right)_N \delta v(r)dr + \int \left(\frac{\partial \delta E}{\partial N \delta v(r)}\right) \delta v(r)dr\Delta N + \frac{1}{2}\iint \left(\frac{\delta^2 E}{\delta v(r)\delta v(r')}\right)\delta v(r)\delta v\left(r'\right)drdr' + \ldots = E^0[N, v(r)] + \mu\Delta N + \eta\Delta N^2 + \int \rho(r)\delta v(r)dr + \int f(r)\delta v(r)dr + \frac{1}{2}\iint \chi(r,r')\delta v(r)\delta v(r')drdr' + \ldots \quad (18)$$

In Eq. 18, the chemical potential (μ) can be interpreted as the tendency to have the electrons leave the electron cloud, whereas the chemical hardness ( ) can be defined as the opposition to have the electrons deform the cloud and finally the linear response funtion (χ(r,r')) [19–21].

The chemical potential can be calculated using the Koopmans' theorem:

$$\mu \approx \frac{\varepsilon_L + \varepsilon_H}{2} \quad (19)$$

where (ε_L) is the energy of the lowest unoccupied molecular orbital (LUMO) and (ε_H) is the energy of the highest occupied molecular orbital (HOMO) [19, 21]. From Eq. (19) it is possible to obtain a quantitative expression for the chemical hardness according to Pearson et al. [31]. Thus, the chemical hardness can be defined as:

$$\eta \approx \varepsilon_L - \varepsilon_H \quad (20)$$

From Eq. (20), we obtain the softness [32], that can be defined as:

$$S = \frac{1}{\eta} \quad (21)$$

The quantities defined in Eqs. (19) and (20) are called global reactivity indexes and provide information about the reactivity or stability of a chemical system [33]. Another important chemical reactivity descriptor is the electrophilicity index (ω) [33, 34]. Electrophilicity index is a measure of the stabilization energy of the system when it is saturated by electrons from the external environment and it is calculated as follows:

$$\omega = \frac{\mu^2}{2\eta} \quad (22)$$

The Fukui function (Eq. 17, *f*) represents the response of the chemical potential of a system to changes in the external potential. It is defined as the derivative of the electronic density with respect to the number of electrons at constant external potential:

$$f_k^+ = \int_k \left[\rho_{N+1}\left(\vec{r}\right) - \rho_N\left(\vec{r}\right)\right] = \left[q_k(N+1) - q_k(N)\right] \quad (23)$$

$$f_k^- = \int_k \left[\rho_N\left(\vec{r}\right) - \rho_{N-1}\left(\vec{r}\right)\right] = \left[q_k(N) - q_k(N-1)\right] \quad (24)$$

where (f_k^+) represents the susceptibility for nucleophilic attack and (f_k^-) represents the susceptibility for electrophilic attack [35–37].

Accordingly, when using the global and local reactivity descriptors, it is possible to study the selectivity on our molecular set.

Molecular set and alignment methods

Molecular set

The molecular set in this study corresponds to a series of bicycle [4.1.0] heptane derivatives as MCH-R1 antagonists. We used the inhibitory activity data (K_i, nM) and the theoretical values, reported by Morales-Bayuelo et al. [26], that are shown in Table 1. These reported results were obtained by a comparative molecular field analysis (CoMFA). Considering the fact that the CoMFA is a 3D QSAR technique based on data from known actives molecules, the molecular fields are calculated around each conformation. The fields that are usually calculated correspond to the electrostatic and steric (van der Waals) interactions. These fields are measured at the lattice points of a regular cartesian 3D grid, where at each grid point, the steric energy (using a Lennard-Jones potential) and the

Table 1 Structures and biological activities in the molecular set

C[a]	NRR'	Exp[b]	CoMFA[c]	
			Pred	Δ
1	1-CH_3 pyrrolidine	7.796	7.915	−0.119
2	2-NHAc pyrrolidine	7.638	7.427	0.211
3	S-2-CH_2OH pyrrolidine	7.824	7.606	0.218
4	R-2-CH_2OH pyrrolidine	8.155	7.749	0.406
5	1-CH_3 piperidine	7.824	7.785	0.039
6	4-CH_3OH piperidine	7.824	7.840	−0.016
7	3-OH piperidine	7.658	7.896	−0.238
8	Azepine	7.824	8.069	−0.245
9	$[(CH_3)_2CH_2)$-$]_2$N-	8.303	8.080	0.223

[a] C: Compound

[b] Exp: Biological activity (nM) expressed as –log *Ki* MCH-R1 antagonists

[c] Note: In order to study the correlation among structure and biological activity, a series of calculations using comparative molecular field analysis (CoMFA) for the novel bioactive bicycle [4.1.0] heptanes analogues were performed. Compounds 1–9 were taken from ref. [26]

electrostatic energy are measured for each molecule by a probe atom (sp^3-hybridized carbon with +1 charge) [38, 39].

The electrostatic and steric molecular fields for the CoMFA were modeled using the quantum similarity and chemical reactivity theoretical frameworks in an effort to get new insights from the well-known CoMFA approach but in the DFT context.

Alignment methods

The MQS has strong dependency on the relative orientation of the structures that are compared. Hence, the criteria for a good superposition are critical. Many methods have been established to create the best conditions for optimal superposition between the compared molecules [40–45]. This work is based on the recognition of the molecular skeleton shown in (Fig. 1b) for the molecular alignment. We assessed the correlation between the quantum similarity and the QSAR models as well [46].

Computational details

All compounds were optimized using a B3LYP (hybrid-GGA exchange-correlation functional) [47–49] at 6-311++G(2d,2p) level of theory. This basis set was used because it has been successful in predicting the geometric, electronic parameters and spectroscopic terms as well as the coupling constants in the nuclear magnetic resonance spectra of aromatic heterocycles involving nitrogen atoms, that is, in good agreement with the experimental results [50]. The same level of theory has been used to calculate the Fukui functions [51, 52]. All the optimizations were carried out using GAUSSIAN 09 [53]. Quantum similarity indexes were calculated using the maximum similarity superposition algorithm (MSSA) [54] and the topo-geometrical superposition algorithm (TGSA) [55] as the molecular alignment methods.

Results and discussion

Local similarity indexes for bicycle [4.1.0] heptane derivatives

Two alignment methodologies, namely MSSA and TGSA, were used in order to determine the quantification of the steric and electronic effects in the bicycle [4.1.0] heptane derivatives as MCH-R1 antagonists. The Tables 1A and 2A in the Supporting information (SI) shows the results for the MSSA method [54], whereas the Tables 3A, 4A, 5A, and 6A (SI) shows the results for the TGSA method [55]. In general, low values in the molecular quantum similarity indexes of overlap were found. The values ranging from (0.0755) to (0.8492), corresponding to the overlap between compounds 7 and 9, and between compounds 2 and 3 respectively, indicate that the alignment method used by the MSSA is not the most appropriate to explain the group correlation reported by the 3D QSAR model [26]. For this reason, the Coulomb index was calculated.

The higher Coulomb index was found between compounds 5 and 6 (0.9825), whereas the lowest value was found between compounds 9 and 7 (0.6426). These Coulomb index values allow to explain the correlation predicted by the steric and electrostatic fields of the CoMFA 3D-QSAR model [26]. The TGSA was used as the alignment method to obtain the structural and electronic descriptors that were used in the study of the pharmaco-kinetics and biological activities associated with the molecular size (see Tables 4A and 5A in SI) [56], taking into account that the molecular size can be eventually an important variable determining the MCH-R1 antagonist activity.

Steric effects in the structures can be related to the overlap index using the quantum molecular alignment of the TGSA method. The higher value was obtained between compounds 8 and 5 (0.9159) with a Euclidean distance of 2.2484, whereas the lowest value was found between compounds 9 and 6 (0.3739) with a Euclidean distance of 6.1980. These values are in agreement with the group correlation (R^2=0.791 and q^2=0.680) reported by the CoMFA 3D QSAR model [26].

In order to get the electrostatic information present in the MCH-R1 antagonists, the electrostatic similarity was

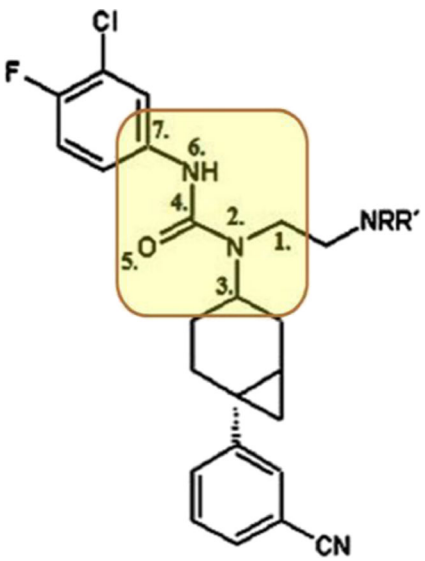

Fig. 2 Electrostatic effects on the molecular bond in the receptor-antagonist sites determined by the substituent NRR' (see Table 1) and reported by Cirauqui et al. [57]

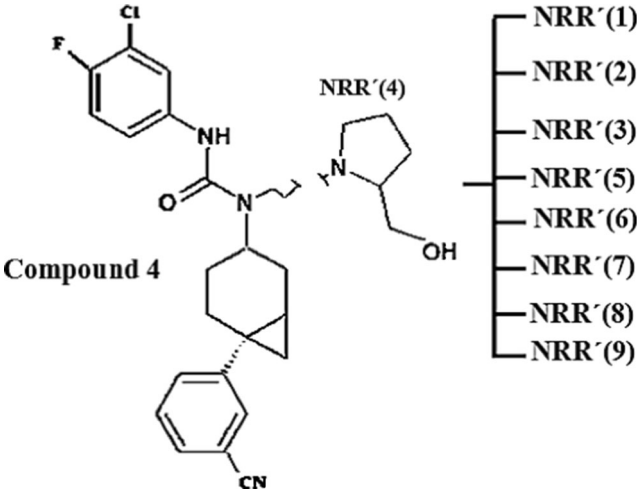

Fig. 3 Relationship scheme of the substituent effects on the overlap and Coulomb scales proposed in this study (see Table 1, where NRR'(4) is the reference compound; NRR'(n) with *n*=Molecular set)

calculated using the Coulomb index, since this index gives information on the local charge distribution and the Coulomb electrostatic repulsion between the charge densities analyzed using the TGSA alignment. The higher value of 0.9956 was obtained between compounds 5 and 6, with a Euclidean distance of 6.7907, indicating that the extra-OH groups in compound 6 with respect to compound 5 have no effect on the electronic distribution. Our results suggest that the electronic descriptors explain the biological activity in a better way than the steric descriptors (see Table 4 in SI). These results are also consistent with the nature of the receptor-antagonist sites that are shown in Fig. 2, according to the molecular model and docking study performed by Cirauqui et al. [57]

In order to perform the quantification of steric and electrostatic effects, we designed the scheme shown in Fig. 3, which depicts the suggested relationships between the substituent effects on the overlap and the Coulomb scales. It is based on a compound with high experimental MCH-R1 antagonist activity and theoretical correlation (compound 4 in Table 1). The Coulomb scale on this scheme takes into consideration the high correlation between the compounds (1–9) determined by Morales-Bayuelo et al. in the CoMFA 3D QSAR model. [26]

Compound 4 was taken as reference for the quantification scales, since it has the higher similarity value from the structural and electrostatic perspective, when it is compared with the compound 1 (see Fig. 4). The same trends are observed for compounds 1, 3, 7, and 9.

In the two scales shown in Fig. 4, the steric and electrostatic substituent effects on the biological activity of the MCH-R1 antagonist can be observed. For instance, the overlap index between compounds 4 and 2 is low (0.4168), whereas the Coulomb index between them is high (0.9489). In this sense, when steric and electrostatic substituent effects are included, these scales may be considered as a possible alternative to the usual drug design techniques, with potential use as new QSAR descriptors.

Global reactivity indexes for bicycle [4.1.0] heptane derivatives

The Coulomb quantum similarity index (see Fig. 4) was the best index found to describe the MCH-R1 antagonist activity with respect to the structural information given by the overlap index. In order to determine how the electrostatic substituent effects determine the receptor-binding, global and local reactivity indexes were used to understand the MCH-R1 antagonists' activity of the protein belonging to the G protein-coupled receptor family 1 and encoded by the MCH-R1 gene [58].

Global reactivity indexes are shown in Table 2. From these data, we can see that compound 9 has the highest value (−2.87 eV) and compound 8 has the lowest value (−3.69 eV) for chemical potential (μ); and that compound 7 has the highest value (4.66 eV), whereas compound 9 has the lowest value (2.95 eV) for chemical hardness (η). Compound 9 also has the highest (0.33 eV) and lowest (4.34 eV) values for chemical softness (S) and ionization potential (IP), respectively.

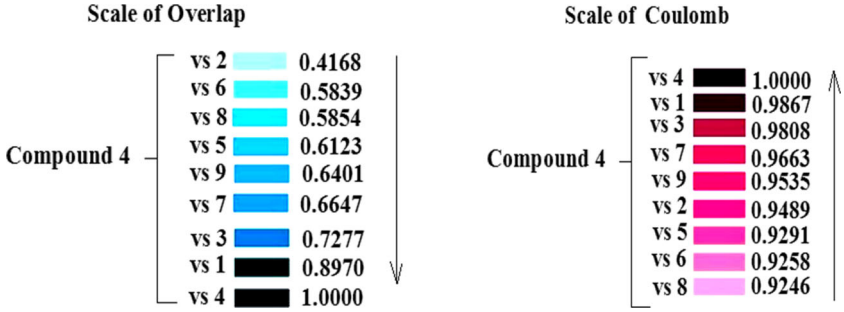

Fig. 4 Quantification scales of steric and electrostatic effects using the topo-geometrical superposition algorithm (TGSA)

Table 2 Global reactivity indexes

Compounds	μ[a] (eV)	η[b] (eV)	S[c](eV^{-1})	IP[d] (eV)	EA[e] (eV)	ω[f] (eV)
1	−3.5749	4.3650	0.2291	5.7574	1.3924	1.4639
2	−3.4924	4.2344	0.2362	5.6096	1.3753	1.4403
3	−3.3911	4.0605	0.2462	5.4213	1.3608	1.4160
4	−3.4361	4.3340	0.2307	5.6031	1.2691	1.3621
5	−3.5342	4.4317	0.2256	5.7500	1.3184	1.4093
6	−3.5653	4.4720	0.2236	5.8600	1.3385	1.4182
7	−3.6567	4.6662	0.2143	5.9898	1.3236	1.4328
8	−3.6987	4.5593	0.2193	5.9783	1.4191	1.5003
9	−2.8707	2.9538	0.3385	4.3476	1.3938	1.3949

[a] μ: chemical potential
[b] η: chemical hardness
[c] S: chemical softness
[d] IP: ionization potential
[e] EA: electron affinity
[f] ω: electrophilicity

Compound 8 has the highest value (1.50 eV) for electrophilicity (ω), i.e., it is the one that better stabilizes the system energy when it is saturated by electrons coming from the receptor, given its chemical potential (μ) and hardness (η).

As commented above, compound 9 is the most reactive in the series according to the global reactivity indexes, that is in agreement with the highest MCH-R1 antagonist activity shown in Table 1 [26]. On the other hand, compound 8 is the less reactive one, in agreement with the high correlation between the chemical reactivity predicted by the CoMFA model [26] and the quantification of steric and electrostatic effects by means of the scales of Fig. 4.

Local reactivity indexes for bicycle [4.1.0] heptane derivatives

Identification of local reactivity sites and selectivity on the substituent NRR' (see Table 1) was achieved in terms of local reactivity indexes. The values for the Fukui function of compound 9 are displayed in Fig. 5 (a). The carbon atom C(11) of compound 9, despite its high susceptibility to nucleophilic attack according to the 0.2526 for its Fukui (f^+(r)) function, it is electronically disabled by the cyano group (−CN$^-$), with Fukui f^+(r) of 0.1170 and 0.1428 for the atoms C (15) and N (16), respectively.

In Fig. 6 (b), the HOMO square surfaces associated with the Fukui function (f^-(r)) belonging to the substituent $[(CH_3)_2CH_2)$-$]_2$N- of compound 9 are shown.

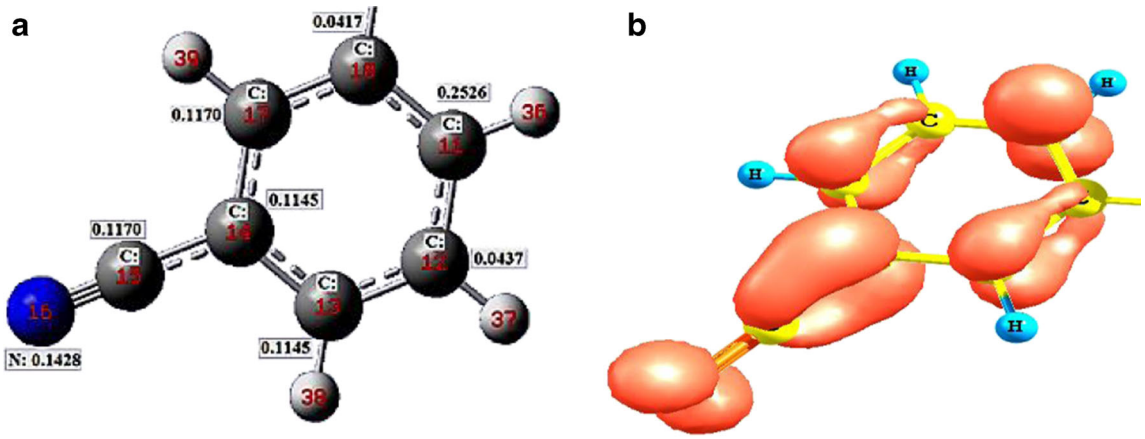

Fig. 5 **a** Condensed Fukui functions (f^+(r)) of compound 9 **b** Surfaces of isovalue 0.005 of the LUMO square (isovalue: 0.0004). Note: this molecular fragment belongs to compound 9 that is the more reactive one according to the global reactivity indexes in Table 2. Note: The Hirshfeld charges are used to compute the condensed Fukui function indices

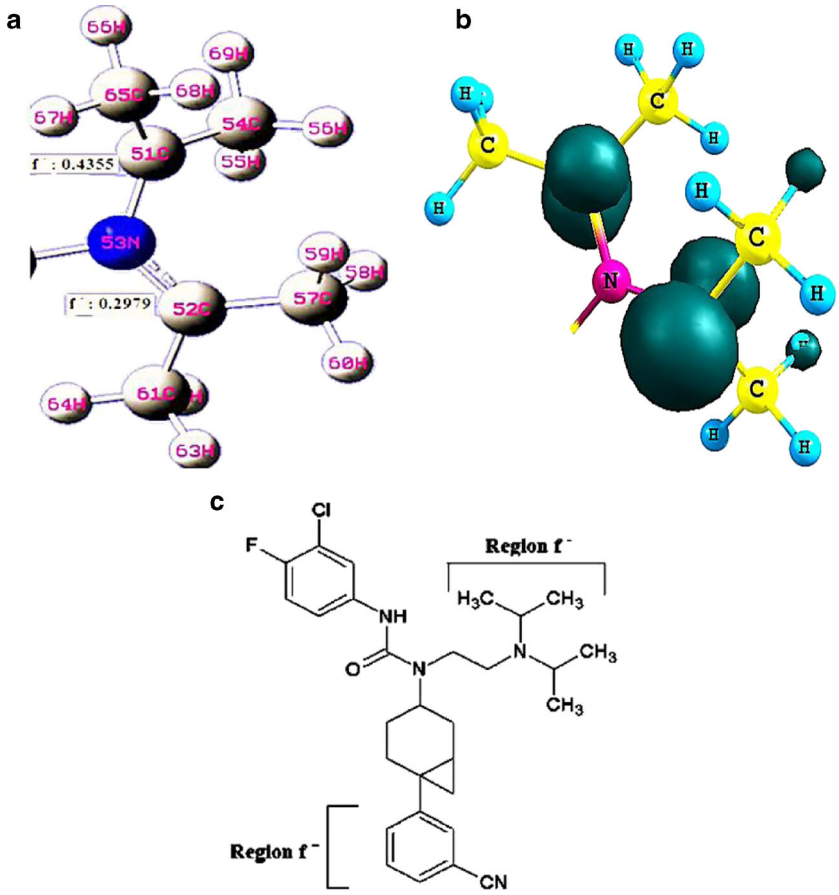

Fig. 6 **a** Molecular fragment for the condensed Fukui functions (f^-(r)) (region f^-). **b** Surfaces: 0.005 of the HOMO square of compound 9 (isovalue: 0.0004) **c** Molecular regions for the corresponding condensed Fukui functions. Note: The region (f^+(r)) is common in all the structures according to Table 1. Note: The Hirshfeld charges are used to compute the condensed Fukui function indices

Despite that compound 9 has the highest chemical reactivity (see Table 2) and that it is the most active MCH-R1 antagonist (with an experimental biological activity of 8.30 nM, see Table 1), compound 4 has considerably high MCH-R1 antagonist activity (with an experimental biological activity of 8.15 nM) and it also has a high group correlation according to Figs. 3 and 4. Hence, condensed Fukui functions (f^-(r)) and the HOMO square surfaces for compound 4 can provide additional information (Fig. 7).

Unlike the condensed Fukui region (f^-(r)) of compound 9, in compound 4 the nitrogen atom N55 of the pyrrolidine group is the most reactive (f^-(r): 0.5730), indicating that such substituent group is the y the quantitative scales of Fig. 4.

Furthermore, the reactivity sites of hydrogen atoms H57 and H63 (Fig. 7b)) suggest susceptibility to form hydrogen bonds with the MCH-R1 receptor as has been previously reported in selectivity studies [58–66].

Conclusions

Since the introduction of the quantum similarity by Carbó-Dorca and coworkers approximately 30 years ago, MQS has been used in studies to relate molecular properties and study correlations in molecular groups with specific activities. Consequently, in this study, we used the quantum similarity field in combination with the chemical reactivity DFT to better understand and interpret the results of 3D-QSAR (CoMFA). In addition, both the electrostatic and steric fields involved in the CoMFA were properly quantified in this work. The quantification of steric and electrostatic effects was based on the MQS field by means of the overlap and Coulomb quantification scales that we have suggested, which allowed to characterize the MCH-R1 antagonist activity according to the electronic distribution determined by steric and electronic effects. We used the topo-geometrical superposition algorithm (TGSA) and the maximum similarity superposition algorithm (MSSA) as alignment methods to deal with the alignment problem in the similarity measures.

Finally, our results are in agreement with the previously reported CoMFA study, showing that the pyrrolidine group is the site with the highest selectivity. Overall, this work suggest that our approach can be used in different QSAR correlation studies and also as a valuable tool in drug design protocols for clinical

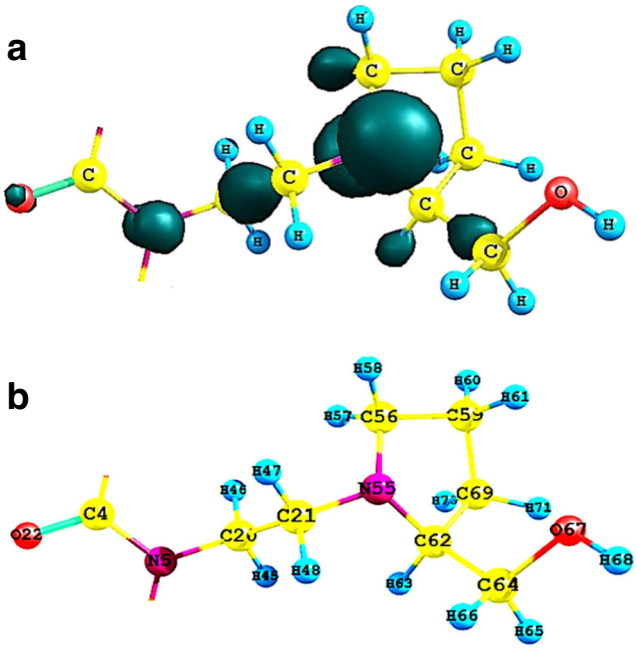

Molecular fragment	$f^-(r)$
5N	0.0777
20C	0.0599
21C	0.0282
22O	0.0203
55N	0.5730
56C	0.0179
57H	0.0499
58H	0.0185
62C	0.0178
63H	0.0342
64C	0.0308

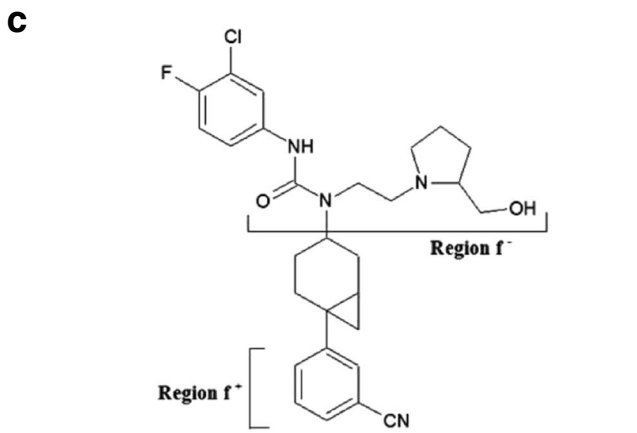

Fig. 7 **a** Surfaces of HOMO square associated with (f^-(r)) of compound 4. **b** Molecular fragment for the condensed Fukui functions f^- (region f^-). **c** Molecular regions for condensed Fukui functions and surfaces: 0.005 of the HOMO square, (isovalue: 0.0004). Note: The region (f^+(r)) is common in all the structures according to Table 1

treatment, in cases when the receptor is known or even when it is not known.

Acknowledgments Thanks to the Universidad de Talca (CBSM)) for the continuous support to this investigation, to the postdoctoral project N^0 3150035 (FONDECYT, CHILE), to Dr. Ramon Carbó-Dorca (Universitat de Girona, España), and finally Dr. Andrzej Sokalski (associate editor) for their important comments.

References

1. Bohm M, Sturzebecher J, Klebe G (1999) J Med Chem 42:458
2. (1999) Nobel lecture: electronic structure of matter—wave functions and density functionals. Rev Mod Phys 71, No. 5
3. Amat L, Carbó-Dorca R, Ponec R (1999) J Med Chem 42:5169
4. Klebe G (1998) Comparative molecular similarity indices: CoMSIA. In: Kubinyi H, Folkers G, Martin YC (eds) 3D QSAR in drug design, vol 3. Kluwer, London, p 87
5. World Health Organization. Obesity and overweight. Consulted January 20, 2014. http://www.who.int/mediacentre/factsheets/fs311/en/index.html. Reported in April 8, 2014.
6. Bleich S, Cutler D, Murray C, Adams A (2008) Annu Rev Public Health 29:273
7. Martinez JA (2000) Body-weight regulation: causes of obesity. Proc Nutr Soc 59:337
8. Bittencourt JC, Presse F, Arias C, Peto C, Vaughan J, Nahon JL, Vale W, Sawchenko PE (1992) J Comp Neurol 319:218
9. Drewnowski A, Specter SE (2004) Am J Clin Nutr 79:6
10. Fernandez-Lopez J, Remesar X, Foz M, Alemany M (2002) For a review of current approaches for the treatment of obesity. Drugs 62: 915
11. James WP (2008) Obes Rev 9:6
12. Nestle M, Jacobson MF (2000) Public Health Rep 115:12
13. Sturm R (2007) Public Health 121:492
14. Wang S, Behan J, O'Neill K, Weig B, Fried S, Laz T, Bayne M, Gustafson E, Hawes BE (2001) J Biol Chem 276:34664
15. Sailer AW, Sano H, Zeng Z, McDonald TP, Pan J, Pong S-S, Feighner SD, Tan CP, Fukami T, Iwaasa H, Hreniuk DL, Morin NR, Sadowski SJ, Ito M, Bansa A, Ky B, Figueroa DJ, Jiang Q, Austin CP, MacNeil DJ, Ishihara A, Ihara M, Kanatani A, Van der Ploeg LHT, Howard AD, Liu Q (2001) Proc Natl Acad Sci 98:7564
16. Chambers J, Ames RS, Bergsma D, Muir A, Fitzgerald LR, Hervieu G, Dytko GM, Foley JJ, Martin J, Liu W-S, Park J, Ellis C, Ganguly S, Cluderay SJ, Leslie RWS, Sarau HM (1999) Nature 400:261
17. Xu R, Li S, Paruchova J, McBriar MD, Guzik H, Palani A, Clader JW, Cox K, Greenlee WJ, Hawes BE, Kowalski TJ, O'Neil K, Spar BD, Weig B, Weston DJ (2006) Bioorg Med Chem 14:3285
18. Amat L, Carbó-Dorca R (2002) Int J Quantum Chem 87:59
19. Geerlings P, De Proft F, Langenaeker W (2003) Chem Rev 103: 1793
20. Parr RG, Yang W (1989) Density Functional Theory of Atoms and Compounds. Oxford University Press, New York
21. Ayers PW, Anderson JSM, Bartolotti LJ (2005) Int J Quantum Chem 101:520
22. Carbó-Dorca R, Arnau M, Leyda L (1980) Int J Quantum Chem 17: 1185
23. Carbó-Dorca R, Gironés X (2005) Int J Quantum Chem 101:8
24. Gironés X, Carbó-Dorca R (2006) QSAR Comb Sci 25:579
25. Bultinck P, Gironés X, Carbó-Dorca R (2005) Rev Comput Chem 21:127
26. Morales-Bayuelo A, Hernan A, Vivas-Reyes R (2010) Eur J Med Chem 45:4509
27. Hirshfeld FL (1977) Theor Chim Acta 44:129
28. De Proft F, Van Alsenoy C, Peeters A, Langenaeker W, Geerlings P (2002) J Comput Chem 23:1198

29. Randic M, Johnson MA, Maggiora GM (1990) In concepts and applications of molecular similarity, design of compounds with desired properties. Wiley, New York. 77.
30. Boon G, Van Alsenoy C, De Proft F, Bultinck P, Geerlings P (2005) J Mol Struct 727:49
31. Pearson RG (1997) Chemical hardness: applications from compounds to solids. Wiley-VHC, Weinheim
32. Yang WT, Parr RG (1985) Proc Natl Acad Sci 82:6723
33. Ayers P, Parr RG (2000) J Am Chem Soc 122:2010
34. Parr RG, Yang W (1984) J Am Chem Soc 106:4049
35. Fuentealba P, Pérez P, Contreras R (2000) J Chem Phys 113:2544
36. Galván M, Pérez P, Contreras R, Fuentealba P (1999) Chem Phys Lett 30:405
37. Mortier WJ, Yang W (1986) J Am Chem Soc 108:5708
38. Blankley CJ (1996) In: van de Waterbeemd H (ed) Structure property correlations in drug research. Academic, Austin, pp 111–177
39. Cramer RD III, Patterson DE, Bunce JD (1988) J Am Chem Soc 110:5959–5967
40. Constans P, Amat L, Carbó-Dorca R (1997) J Comput Chem 18: 826
41. Girones X, Robert D, Carbó-Dorca R (2001) J Comput Chem 22: 255
42. Morales-Bayuelo A, Torres J, Vivas-Reyes R (2012) J Theor Comput Chem 11:1
43. Morales-Bayuelo A, Vivas-Reyes R (2013) J Math Chem 51:125
44. Morales-Bayuelo A, Vivas-Reyes R (2014) J Quant Chem Article ID 239845, 19 pages
45. Morales-Bayuelo A, Vivas-Reyes R (2014) J Quant Chem Article ID 850163, 12 pages
46. Besalú E, Gironés X, Amat L, Carbó-Dorca R (2002) Acc Chem Res 35:289
47. Becke AD (1988) Phys Rev A 38:3098
48. Lee C, Yang W, Parr RG (1988) Phys Rev B 37:785
49. Vosko SH, Wilk L, Nusair M (1980) Can J Phys 58:1200
50. Katritzky AR, Akhmedov NG, Doskocz J, Mohapatra PP, Hall D, Güven A (2007) Magn Reson Chem 45:532
51. Bultinck P, Clarisse D, Ayers P, Carbó-Dorca R (2011) Phys Chem Chem Phys 13:6110
52. Morales-Bayuelo A, Caballero J (2015) J Mol Model 21:45
53. Frisch MJ, G. Trucks W, Schlegel HB, Scuseria GE, Robb MA, Cheeseman JR, Scalmani G, Barone V, Mennucci B, Petersson GA, Nakatsuji H, Caricato M, Li X, Hratchian HP, Izmaylov AF, Bloino J, Zheng G, Sonnenberg JL, Hada M, Ehara M, Toyota K, Fukuda R, Hasegawa J, Ishida M, Nakajima T, Honda Y, Kitao O, Nakai H, Vreven T, Jr. Montgomery JA, Peralta JE, Ogliaro F, Bearpark M, Heyd JJ, Brothers E, Kudin KN, Staroverov VN, Keith T, Kobayashi R, Normand J, Raghavachari K, Rendell A, Burant JC, Iyengar SS, Tomasi J, Cossi M, Rega N, Millam JM, Klene M, Knox JE, Cross JB, Bakken V, Adamo C, Jaramillo J, Gomperts R, Stratmann RE, Yazyev O, Austin AJ, Cammi R, Pomelli C, Ochterski JW, Martin RL, Morokuma K, Zakrzewski VG, Voth GA, Salvador P, Dannenberg JJ, Dapprich S, Daniels AD, Farkas O, Foresman JB, Ortiz JV, Cioslowski J, Fox DJ (2010) Gaussian 09, Revision C.01. Gaussian Inc, Wallingford, CT
54. Constans P, Amat L, Carbó-Dorca R (1997) J Comput Chem 18: 826
55. Girones X, Robert D, Carbó-Dorca R (2001) J Comput Chem 22: 255
56. Dyck B, Markison S, Zhao L, Tamiya J, Grey J, Rowbottom MW, Zhang M, Vickers T, Sorensen K, Norton C, Wen J, Heise CE, Saunders J, Conlon P, Madan A, Schwarz D, Goodfellow VS (2006) J Med Chem 49:3753
57. Cirauqui N, Schrey AK, Galiano S, Ceras J, Pérez-Silanes S, Aldana I, Monge A, Kühne R (2010) Bioorg Med Chem 18:7365
58. MCH-R1 melanin-concentrating hormone receptor 1 (Homo sapiens). http://www.ncbi.nlm.nih.gov/sites/entrez Gene ID: 2847, updated on 14-01-2015
59. Cheon HG (2012) Handb Exp Pharmacol 209:383
60. Hervieu G (2003) Expert Opin Ther Targets 7:495
61. Hervieu GJ (2006) Expert Opin Ther Targets 10:211
62. Huttunen R, Syrjänen J (2013) Int J Obes 37:333
63. Rivera G, Bocanegra-García V, Galiano S, Cirauqui N, Ceras J, Pérez S, Aldana I, Monge A (2008) Curr Med Chem 15:1025
64. Saito Y, Maruyama K (2006) J Exp Zool Comp Exp Biol 305:761
65. Shimazaki T, Yoshimizu T, Chaki S (2006) CNS Drugs 20:801
66. Su J, McKittrick BA, Tang H, Czarniecki M, Greenlee WJ, Hawes BE, O'Neill K (2005) Bioorg Med Chem 5:1829